







RESEARCH ARTICLE | FEBRUARY 29 2024

Magnons in a two-dimensional Weyl magnet

Special Collection: [Magnonics](#)

Ying-Jiun Chen  ; Tzu-Hung Chuang  ; Jan-Philipp Hanke; Yuriy Mokrousov  ; Stefan Blügel  ;
Claus M. Schneider  ; Christian Tüsche 



Appl. Phys. Lett. 124, 093105 (2024)

<https://doi.org/10.1063/5.0195222>




View
Online




Export
Citation


CrossMark



Lock-in Amplifier



Boxcar Averager



Zurich
Instruments

Find out more

Boost Your Optics and
Photonics Measurements

Magnons in a two-dimensional Weyl magnet

Cite as: Appl. Phys. Lett. **124**, 093105 (2024); doi: [10.1063/5.0195222](https://doi.org/10.1063/5.0195222)

Submitted: 31 December 2023 · Accepted: 4 February 2024 ·

Published Online: 29 February 2024



View Online



Export Citation



CrossMark

Ying-Jiun Chen,^{1,2,a)}  Tzu-Hung Chuang,³  Jan-Philipp Hanke,^{2,4}  Yuriy Mokrousov,^{2,4,5}  Stefan Blügel,^{2,4} 
Claus M. Schneider,^{2,6,7}  and Christian Tuschke^{2,6,a)} 

AFFILIATIONS

¹Ernst Ruska-Centre for Microscopy and Spectroscopy With Electrons, Forschungszentrum Jülich, 52425 Jülich, Germany

²Peter Grünberg Institut, Forschungszentrum Jülich, 52425 Jülich, Germany

³National Synchrotron Radiation Research Center, Hsinchu 300092, Taiwan

⁴Institute for Advanced Simulation, Forschungszentrum Jülich and JARA, 52425 Jülich, Germany

⁵Institute of Physics, Johannes Gutenberg University Mainz, 55099 Mainz, Germany

⁶Fakultät für Physik, Universität Duisburg-Essen, 47057 Duisburg, Germany

⁷Department of Physics, University of California Davis, Davis, California 95616, USA

Note: This paper is part of the APL Special Collection on Magnonics.

a) Authors to whom correspondence should be addressed: yi.chen@fz-juelich.de and c.tuschke@fz-juelich.de

ABSTRACT

The discovery of topological states of matter has led to a revolution in condensed-matter science. While a non-trivial band topology in a material is often associated with intriguing transport properties, much less attention has been given to the impact on spin dynamics and non-equilibrium magnetization states. Here, we provide evidence that a chiral asymmetric magnon dispersion in the two-dimensional Weyl magnet Fe/W(110) is related to the presence of Weyl fermions close to the Fermi energy and surface Fermi arcs. We find that the large anomalous Hall conductivity and the Dzyaloshinskii–Moriya interaction are attributed to the non-trivial band topology in the composite momentum-magnetization space. Our results show the direct impact of Weyl fermions on both the charge and spin dynamics in a two-dimensional magnet. Unveiling these principles can promote innovative technologies in magnonics by utilizing topological materials, where magnons and non-trivial topological electronic states can be manipulated through magnetization.

© 2024 Author(s). All article content, except where otherwise noted, is licensed under a Creative Commons Attribution (CC BY) license (<http://creativecommons.org/licenses/by/4.0/>). <https://doi.org/10.1063/5.0195222>

The electron spin, a fundamental quantum mechanical property, is pivotal in determining the electronic and magnetic properties as well as the dynamics of matter.^{1–3} In magnetic materials, magnons describe the elementary excitation of a macroscopically ordered ground-state spin configuration, and their excitation allows the transfer of spin angular momentum without involving charge transport. The fundamental understanding of magnons, thus, holds significant importance for both fundamental science and modern applications, particularly in the emerging field of magnonics.^{4–8} Magnonic devices for data processing and computation have the potential to operate with minimal charge-related dissipation.^{4,5} Notably, magnons dominated by exchange interaction, with nanometer wavelengths reaching into the THz frequency range, address key demands in modern computing, such as downsizing, ultrafast operation, and energy-efficient data processing at room temperature.^{4,9}

A basic description of magnons and their energy dispersion as a function of the wave vector is based on the spin Hamiltonian,

incorporating a Heisenberg spin model and the Dzyaloshinskii–Moriya (DM) interaction. While these models indirectly account for local magnetic exchange and spin–orbit interaction, their applicability is limited to some extent when dealing with itinerant magnetic materials. In such cases, the microscopic magnetic parameters are governed by the underlying electronic structures.^{9–12} Examples are spin-dependent electron correlations in the electronic structure of itinerant ferromagnets that alter the magnon dispersion but also defeat the general picture of a rigid exchange splitting of the electronic states.^{2,9} Recently, the role of a non-trivial band topology came into focus for explaining spin-dependent non-equilibrium properties, such as the anomalous Hall conductivity (AHC), and magnon spectra in topological magnetic materials.^{13–18} For instance, an anomalous temperature dependence of the magnon gap in the topological magnetic material SrRuO₃, together with a large AHC, has been attributed to the appearance of Weyl fermions.^{15,16}

In ultrathin iron films on W(110), an asymmetric magnon dispersion has been observed and attributed to the presence of the DM

interaction.^{19,20} Remarkably, in the same system, the presence of topological Weyl fermions and Fermi arcs has been recently reported.³ Such Weyl fermions display a monopole-like distribution of the Berry curvature, representing a fictitious magnetic field in momentum-space and inducing an anomalous velocity in the motion of electrons in real space. As a result, it is expected that Weyl monopoles will possess strong impact on charge transport, such as the anomalous Hall effect.^{13,14} While the intrinsic mechanism of chiral asymmetric magnon spectra has been interpreted by the notions of DM interaction, their microscopic origin and the role of Weyl fermions have remained elusive.

In this Letter, we unveil an important imprint of Weyl fermions on both magnetic dynamics and transport properties. We focus on the two-dimensional (2D) Weyl ferromagnet that consists of two monolayers (MLs) of Fe with in-plane magnetization, grown epitaxially on a W(110) substrate. Fermi arc states that emerge from the Weyl fermions along the $\bar{\Gamma} - \bar{H}$ direction in the surface Brillouin zone act as sources of both a large AHC and DM interaction. The region of such non-trivial states corresponds to the maximum difference in magnon energies in momentum space and intersect with the magnon propagation direction. Our results show that the presence of Weyl fermions and surface Fermi arcs plays a crucial role on the magnon excitations and AHC.

To investigate magnon dispersions in thin magnetic films, we employ spin-polarized high-resolution electron energy-loss spectroscopy (SPEELS). This technique allows for the measurement of magnetic excitations, providing spin, energy, and momentum resolution across the whole surface Brillouin zone of low-dimensional magnets.^{9,21} A schematic representation of the scattering geometry is given in Fig. 1(a). In the SPEELS experiments, the intensity of the inelastically scattered electrons is recorded for incident electrons of opposite spin polarization, denoted as I_{down} and I_{up} spectra. Figure 1(c) shows typical SPEELS spectra measured at $\Delta K_x = 0.7 \text{ \AA}^{-1}$. I_{down} and I_{up} spectra are referred to the measured intensities of scattered electrons when the spin polarization vector of the incoming electron beam is parallel and antiparallel to the $\bar{\Gamma} - \bar{N}$ direction (the magnetic easy axis of the Fe film), respectively. All the information regarding the energies of the magnons is obtained by analyzing the difference spectra $I_{\text{down}} - I_{\text{up}}$, shown as green circles in Fig. 1(c). The dispersion relation is constructed by plotting the magnon energy vs ΔK_x .^{5,9,21,22}

The measurements were performed for the magnetization parallel and antiparallel to the $\bar{\Gamma} - \bar{N}$ direction, denoted by M_{+y} and M_{-y} , and are summarized in Fig. 1(d). As shown in Fig. 1(d), the magnon dispersion relation is split into two branches for a magnetization along two opposite directions, meaning that the magnon energies with wave vectors of equal magnitude and opposite directions are no longer degenerate. The angular momentum of a given magnon mode can be associated with its handedness. Theory recently predicts that the chiral degeneracy of magnons in ultrathin magnetic films can be lifted, due to the presence of the DM interaction.^{19,23–25}

In order to investigate the electronic origin of the asymmetric magnon dispersion, we performed momentum microscopy experiments on two MLs of Fe on W(110) for both magnetization orientations, parallel and anti-parallel to the $\bar{\Gamma} - \bar{N}(y)$ direction as denoted by M_{+y} and M_{-y} , respectively. Figure 2(a) presents the principal layout of the experimental geometry for our spin-resolved photoemission study. The momentum microscope simultaneously collects

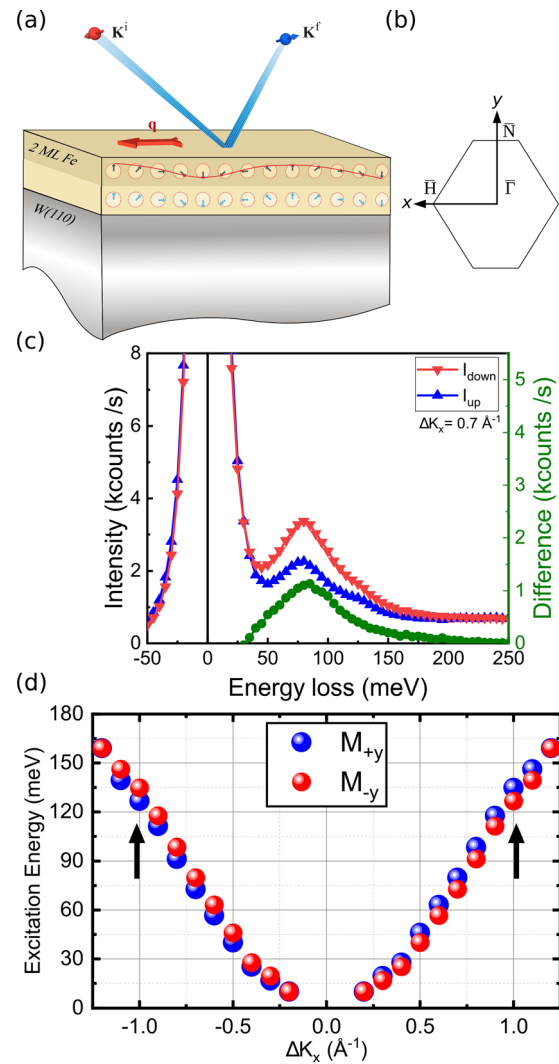


FIG. 1. Measured chiral asymmetric magnon dispersion in a two MLs of Fe on W(110). (a) Schematic representation of the SPEELS experiment. Magnons are excited by incidence of electrons of minority character. K^i and K^f are the momenta of electrons before and after the scattering process, respectively. $q = \Delta K$ is the momentum of excited magnons. (b) Sketch of the surface Brillouin zone of a bcc (110) plane. The high symmetry points of the surface Brillouin zone are labeled. (c) Typical spin polarized electron energy loss spectra recorded on two MLs of Fe on W(110) at a wave-vector transfer of $\Delta K_x = 0.7 \text{ \AA}^{-1}$. The difference spectrum ($I_{\text{diff}} = I_{\text{down}} - I_{\text{up}}$) is shown as green circles. (d) Measured magnon dispersion relation on a two MLs of Fe on W(110) for the magnetization parallel and antiparallel to the $\bar{\Gamma} - \bar{N}$ direction, as denoted by M_{+y} and M_{-y} . The arrow marks the position of the surface Fermi arcs.

photoelectrons over the full solid angle above the sample, such that spin- and momentum-resolved photoemission experiments over the whole Brillouin zone can be performed.^{3,26–28} Combined with the recent groundbreaking invention of imaging spin detection,^{27,29} this approach offers full access to detailed spin-resolved Fermi surfaces that were previously inaccessible by conventional photoelectron spectroscopy.^{30,31}

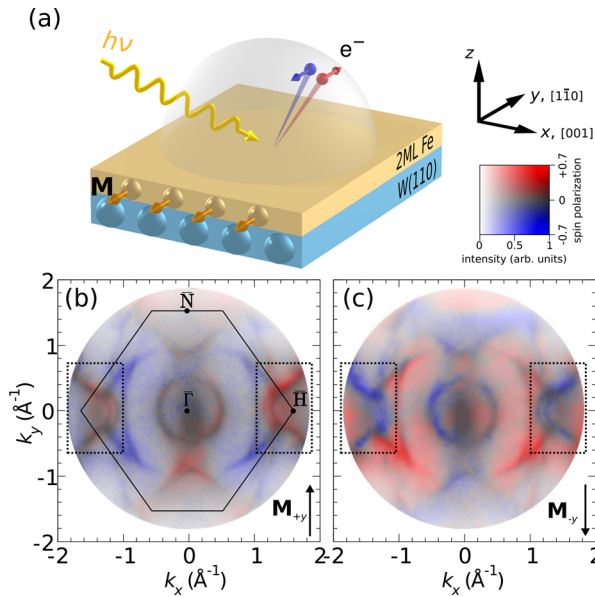


FIG. 2. (a) Experimental geometry for the spin- and momentum-resolved photoelectron study of the Fermi surface. The magnetization \mathbf{M} and the spin polarization P_y are oriented in-plane along the y axis, i.e., the crystallographic bcc $[110]$ direction. (b) and (c) Spin-resolved photoemission momentum maps at the Fermi energy E_F for two MLs of Fe films grown on W(110), measured with a photon energy of $h\nu = 50$ eV for a sample magnetization pointing into $+y$ (b) $-y$ (c) direction. The shape and the spin polarization of the strongly asymmetric Fermi arcs on opposite sides of the momentum map is interchanged if the magnetization direction is reversed. The spin polarization P_y is indicated by red and blue colors, and the color strength encodes the intensity.

Figure 2(b) and 2(c) show the spin-resolved momentum map that we obtain at the Fermi energy, revealing the appearance of prominent surface states in the highlighted regions on both sides of the momentum map. These open arcs with a crescent-moon shape exhibit a high spin polarization. The sign of their spin polarization P_y changes upon magnetization reversal as the surface arc topology is interchanged between the two sides of the momentum map. Among all states at the Fermi surface, the open arcs show the most striking asymmetry of the photoemission intensity and the shape between the left and right side of the momentum map. Such magnetization-dependent asymmetries require the presence of spin-orbit coupling, mediated through hybridization with substrate states in the regions of the Fermi arcs. The pronounced k -dependent relativistic splitting is promoted by both, the broken TR symmetry and missing spatial inversion symmetry at the interface. This mechanism is reminiscent of the physical process that gives rise to the interfacial DMI, as evidenced by previous findings of an asymmetric magnon dispersion in this system.^{19,20,23,32}

The measured band dispersions with degeneracy points appear at a slightly lower binding energy of 200 meV below the Fermi level, which are associated with Weyl fermions in a composite phase space (k_x, k_y, \mathbf{m}) , where \mathbf{m} denotes the magnetization direction of the film. The Fermi arcs, that are observed in the $k_x - k_y$ plane, connect the projection of the mixed Weyl fermions³ and are expected to significantly contribute to magneto-transport properties such as the anomalous Hall conductivity (AHC) of the film.^{13,14}

To better understand how the emergence of band crossings (or monopoles) in the electronic structure relates to spin dynamics and magneto-transport properties in a two-dimensional magnet, we perform advanced first-principles calculations to evaluate the AHC and DM interaction in the composite phase space of crystal momentum and magnetization direction, based on a higher-dimensional Wannier interpolation.^{10,14}

Figure 3(b) presents the resulting momentum-resolved distribution of the microscopic origin of DM interaction, summed over all occupied bands in the highlighted regions of (a), considering the differences in magnetization between M_{+y} and M_{-y} . While many regions in the DM interaction exhibit inversion at opposite crystal momenta, leading to a cancelation and, consequently, a negligible net effect, it is important to note that the mixed Weyl fermions at the end points of the Fermi arcs (marked by the yellow and green circles) play a substantial role in contributing to the total DM interaction and thus chiral asymmetric magnons.

Unveiling the response of the electronic structure to the spin dynamics holds bright promises for understanding various magneto-transport phenomena such as the anomalous Hall conductivity. It has been observed that the mixed Weyl fermions near the end points of the Fermi arcs induce hot-spots in the Berry curvature.³ Recent studies indicate that the strength of AHC is closely related to the Berry curvature of the occupied electronic Bloch states.¹⁴ Figure 3(a) shows that the emergent Weyl fermions and surface Fermi arcs contribute

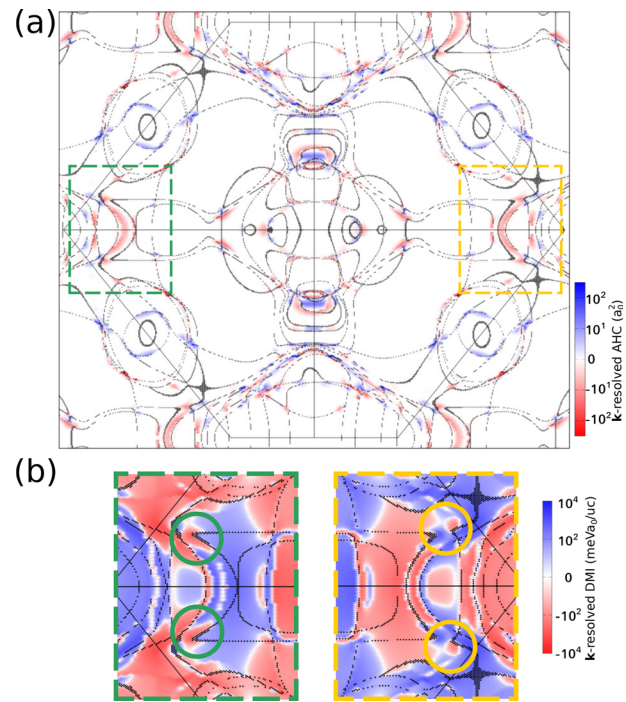


FIG. 3. Momentum distribution of (a) theoretical anomalous Hall conductivity (AHC) and (b) Dzyaloshinskii-Moriya (DM) interaction of all occupied bands throughout the whole surface Brillouin zone for the differences in magnetization between M_{+y} and M_{-y} . The calculated electronic states around the Fermi energy are represented by gray lines. The yellow and green circles in (b) highlight the magnified role of mixed Weyl fermions in the DM interaction.

significantly to the total of AHC in the system. The intrinsic anomalous Hall effect describes the linear response to an applied electric field in terms of an induced current $\mathbf{J} = \sigma \mathbf{E}$ that roots purely in the geometrical properties of the d -dimensional phase space as encoded in the Berry curvature $\Omega_{ij}^n(\mathbf{k})$. The total of the AHC is given by $\sigma_{ij} = \frac{e^2}{h} \int \sum_n^{\text{occ}} \Omega_{ij}^n(\mathbf{k}) \frac{d^d k}{(2\pi)^d}$. The emergence of the anomalous Hall effect can be understood as a direct consequence of the magnetic monopoles acting as sources of the Berry curvature in momentum space, which is visible in the momentum-space distributions of the AHC. We note that the maximum difference in magnon energies between M_{+y} and M_{-y} occurs at about $\Delta K_x = 1.0 \text{ \AA}^{-1}$ [see arrows in Fig. 1(d)]. This region corresponds to the location of magnetic monopoles and surface Fermi arcs in the 2D photoemission momentum map.

To conclude, we have studied a full picture of magnon dispersion, spin-resolved Fermi surface, anomalous Hall effect, and Dzyaloshinskii-Moriya interaction in a two-dimensional magnetic Weyl material. The magnon modes exhibit chiral asymmetric dispersions, such that the energies of magnons with opposite wave vectors are no longer degenerate. This finding can be explained by the presence of emergent monopoles in the composite momentum-magnetization space $(k_x, k_y, \hat{\mathbf{m}})$, so-called mixed Weyl nodes, close to the Fermi energy. Such Weyl nodes possess a significant impact on the anomalous Hall effect and DM interaction. The latter leads to the origin of a chiral symmetric magnon dispersion in a two-dimensional magnet. Our results show that the presence of Weyl nodes close to the Fermi energy plays a crucial role on the magnon excitation and AHC. Uncovering these principles can promote innovative technologies based on magnonics in topological materials, where magnons and non-trivial topological states are controlled on demand through magnetization.

Y.-J.C. and C.T. thank the staff of Elettra for their help and hospitality during their visit in Trieste, and beamline staff M. Jugovac, G. Zamborlini, V. Feyer (PGI-6, FZ-Jülich), and T. O. Menteş (Elettra) for their assistance during the experiment. We are indebted to Kh. Zakeri, Y. Zhang, and J. Kirschner for discussions. Y.-J.C., C.T., and C.M.S. gratefully acknowledge funding by the BMBF (Grant No. 05K19PGA). T.-H.C. acknowledges funding by the National Science and Technology Council of Taiwan (Grant No. NSTC 112-2112-M-213-015). Y.M. acknowledges support by the Deutsche Forschungsgemeinschaft (DFG, German Research Foundation)-TRR 288-422213477 (project B06). We also gratefully acknowledge the Jülich Supercomputing Centre and RWTH Aachen University for providing computational resources under projects cjjf40 and jara0062.

AUTHOR DECLARATIONS

Conflict of Interest

The authors have no conflicts to disclose.

Author Contributions

Ying-Jiun Chen: Conceptualization (equal); Data curation (equal); Formal analysis (equal); Investigation (equal); Methodology (equal); Validation (equal); Visualization (equal); Writing – original draft (equal); Writing – review & editing (equal). **Tzu-Hung Chuang:** Data curation (equal); Formal analysis (equal); Investigation (equal);

Methodology (equal); Visualization (equal); Writing – original draft (equal); Writing – review & editing (equal). **Jan-Philipp Hanke:** Data curation (equal); Formal analysis (equal); Investigation (equal); Software (equal); Visualization (equal); Writing – review & editing (equal). **Yuriy Mokrousov:** Methodology (equal); Resources (equal); Software (equal); Supervision (equal); Validation (equal); Writing – review & editing (equal). **Stefan Blügel:** Conceptualization (equal); Resources (equal); Supervision (equal); Validation (equal); Writing – review & editing (equal). **Claus M. Schneider:** Conceptualization (equal); Funding acquisition (equal); Resources (equal); Supervision (equal); Validation (equal); Writing – review & editing (equal). **Christian Tusche:** Conceptualization (equal); Funding acquisition (equal); Investigation (equal); Methodology (equal); Resources (equal); Supervision (equal); Validation (equal); Writing – original draft (equal); Writing – review & editing (equal).

DATA AVAILABILITY

The data that support the findings of this study are available from the corresponding authors upon reasonable request.

REFERENCES

- Walowski and M. Münzenberg, *J. Appl. Phys.* **120**, 140901 (2016).
- C. Tusche, M. Ellguth, V. Feyer, A. Krasnyuk, C. Wiemann, J. Henk, C. M. Schneider, and J. Kirschner, *Nat. Commun.* **9**, 3727 (2018).
- Y.-J. Chen, J.-P. Hanke, M. Hoffmann, G. Bihlmayer, Y. Mokrousov, S. Blügel, C. M. Schneider, and C. Tusche, *Nat. Commun.* **13**, 5309 (2022).
- A. V. Chumak, P. Kabos, M. Wu, C. Abert, C. Adelman, A. Adeyeye, J. Åkerman, F. G. Aliev, A. Anane, A. Awad *et al.*, *IEEE Trans. Magn.* **58**, 0800172 (2022).
- A. V. Chumak, A. A. Serga, and B. Hillebrands, *Nat. Commun.* **5**, 4700 (2014).
- J. C. Gartside, K. D. Stenning, A. Vanstone, H. H. Holder, D. M. Arroo, T. Dion, F. Caravelli, H. Kurebayashi, and W. R. Branford, *Nat. Nanotechnol.* **17**, 460 (2022).
- P. Chen, H. Wang, C. Cheng, C. Wan, D. Zhang, Y. Wang, Y. Wang, W. He, B. Chi, Y. Liu *et al.*, *Phys. Rev. Appl.* **20**, 054019 (2023).
- Y. Cheng, K. Chen, and S. Zhang, *Appl. Phys. Lett.* **112**, 052405 (2018).
- Y.-J. Chen, K. Zakeri, A. Ernst, H. J. Qin, Y. Meng, and J. Kirschner, *Phys. Rev. Lett.* **119**, 267201 (2017).
- J.-P. Hanke, F. Freimuth, S. Blügel, and Y. Mokrousov, *J. Phys. Soc. Jpn.* **87**, 041010 (2018).
- V. Borisov, Y. O. Kvashnin, N. Taltis, D. Thonig, P. Thunström, M. Pereiro, A. Bergman, E. Sjöqvist, A. Delin, L. Nordström *et al.*, *Phys. Rev. B* **103**, 174422 (2021).
- S. Paischer, G. Vignale, M. I. Katsnelson, A. Ernst, and P. A. Buczek, *Phys. Rev. B* **107**, 134410 (2023).
- S. Ghosh, P. Rüßmann, Y. Mokrousov, F. Freimuth, and A. Kosma, *J. Appl. Phys.* **133**, 230901 (2023).
- J.-P. Hanke, F. Freimuth, C. Niu, S. Blügel, and Y. Mokrousov, *Nat. Commun.* **8**, 1479 (2017).
- S. Itoh, Y. Endoh, T. Yokoo, S. Ibuka, J.-G. Park, Y. Kaneko, K. S. Takahashi, Y. Tokura, and N. Nagaosa, *Nat. Commun.* **7**, 11788 (2016).
- K. Jenni, S. Kunkemöller, D. Brünig, T. Lorenz, Y. Sidis, A. Schneidewind, A. A. Nugroho, A. Rosch, D. I. Khomskii, and M. Braden, *Phys. Rev. Lett.* **123**, 017202 (2019).
- N. Nagaosa, T. Morimoto, and Y. Tokura, *Nat. Rev. Mater.* **5**, 621 (2020).
- J. Wei, H. Zhong, J. Liu, X. Wang, F. Meng, H. Xu, Y. Liu, X. Luo, Q. Zhang, Y. Guang *et al.*, *Adv. Funct. Mater.* **31**, 2100380 (2021).
- L. Udvardi and L. Szunyogh, *Phys. Rev. Lett.* **102**, 207204 (2009).
- K. Zakeri, Y. Zhang, J. Prokop, T.-H. Chuang, N. Sakr, W. X. Tang, and J. Kirschner, *Phys. Rev. Lett.* **104**, 137203 (2010).
- R. Vollmer, M. Etzkorn, P. A. Kumar, H. Ibach, and J. Kirschner, *J. Magn. Magn. Mater.* **272–276**, 2126 (2004).

- ²²T.-H. Chuang, K. Zakeri, A. Ernst, L. M. Sandratskii, P. Buczek, Y. Zhang, H. J. Qin, W. Adeagbo, W. Hergert, and J. Kirschner, *Phys. Rev. Lett.* **109**, 207201 (2012).
- ²³A. T. Costa, R. B. Muniz, S. Lounis, A. B. Klautau, and D. L. Mills, *Phys. Rev. B* **82**, 014428 (2010).
- ²⁴F. J. dos Santos, M. dos Santos Dias, and S. Lounis, *Phys. Rev. B* **102**, 104401 (2020).
- ²⁵M. Kuepferling, A. Casiraghi, G. Soares, G. Durin, F. Garcia-Sanchez, L. Chen, C. H. Back, C. H. Marrows, S. Tacchi, and G. Carloti, *Rev. Mod. Phys.* **95**, 015003 (2023).
- ²⁶Y.-J. Chen, M. Hoffmann, B. Zimmermann, G. Bihlmayer, S. Blügel, C. M. Schneider, and C. Tusche, *Commun. Phys.* **4**, 179 (2021).
- ²⁷C. Tusche, A. Kasyuk, and J. Kirschner, *Ultramicroscopy* **159**, 520 (2015).
- ²⁸C. Tusche, Y.-J. Chen, C. M. Schneider, and J. Kirschner, *Ultramicroscopy* **206**, 112815 (2019).
- ²⁹C. Tusche, M. Ellguth, A. Ünal, C.-T. Chiang, A. Winkelmann, A. Kasyuk, M. Hahn, G. Schönhense, and J. Kirschner, *Appl. Phys. Lett.* **99**, 032505 (2011).
- ³⁰S. Suga and C. Tusche, *J. Electron Spectrosc. Relat. Phenom.* **200**, 119 (2015).
- ³¹C. Tusche, Y.-J. Chen, L. Plucinski, and C. M. Schneider, *e-J. Surf. Sci. Nanotechnol.* **18**, 48 (2020).
- ³²K. Zakeri, Y. Zhang, T.-H. Chuang, and J. Kirschner, *Phys. Rev. Lett.* **108**, 197205 (2012).